doi:10.1006/jmbi.2000.3682 available online at http://www.idealibrary.com on IDEAL® J. Mol. Biol. (2000) 299, 725–735

JMB

A Genetic Analysis of Crystal Growth

Stanley Brown[1]*, Mehmet Sarikaya[2] and Erik Johnson[3]

[1]*Department of Molecular Cell Biology, University of Copenhagen, Øster Farimagsgade 2A, DK-1353, Copenhagen K, Denmark*

[2]*Department of Materials Science and Engineering University of Washington Seattle, WA 98195, USA*

[3]*Niels Bohr Institute, Ørsted Laboratory, University of Copenhagen, Universitetsparken 5, DK-2100, Copenhagen Ø Denmark*

**Corresponding author*

The regulation of crystal morphology by proteins is often observed in biology. It is a central feature in the formation of hard tissues such as bones, teeth and mollusc shells. We have developed a genetic system in the bacterium *Escherichia coli* to study the protein-mediated control of crystal growth. We have used the crystallization of gold as a model system and found polypeptides that control the morphology of the resulting gold crystals. Analysis of the crystallization process influenced by these polypeptides indicates they act catalytically by an acid mechanism. Our results suggest that the concepts and methods of microbial genetics are general and can be applied to substances not commonly found in biological systems.

Keywords: gold; crystal morphology; peptide display

Introduction

Proteins catalyze a vast array of reactions. Analysis of enzymes and the reactions they catalyze has led to an improved understanding of biological processes. Genetic and biochemical analyses have been applied primarily to chemical processes known to mediate biological functions. None-theless, strategies that have been developed to study biological reactions should be generally applicable to reactions able to occur in physiological conditions. The formation of metallic gold, an exceptionally well-studied process (Turkevich *et al.*, 1951; Handley, 1989), meets this criterion.

Metallic gold is relatively inert and is stable in water. Although binding to metallic gold by many proteins requires protein concentrations exceeding 0.1 μM (Geddes *et al.*, 1994), proteins able to adhere efficiently at one-thousandth that concentration can be isolated by genetic selection (Brown, 1997). Furthermore, gold can be reduced from $AuCl_3$ at neutral pH and room temperature by mild reducing agents such as ascorbic acid, vitamin C (Stathis & Fabrikanos, 1958). Gold, when reduced from $AuCl_3$, changes the color of the solution from pale yellow to a red colloid (reviewed by Turkevich *et al.*, 1951). This provides a simple method for monitoring the rate and extent of crystallization. Thus, the crystallization of gold permits selections and screens amenable to analysis by bacterial genetics.

Individual proteins and protein fractions are able to regulate crystal growth in mollusc shells (for example, see Falini *et al.*, 1996; Belcher *et al.*, 1996). Independently, genetic analyses have identified proteins (Brown, 1992; Barbas *et al.*, 1993) and repeating polypeptides (Brown, 1997) that adhere specifically to inorganic surfaces. Thus, it would not be surprising if repeating polypeptides could be found that regulate the morphology of other inorganic crystals.

The isolation of functional peptides from random populations often requires more than one step (reviewed by Wells, 1996). This is probably because the number of amino acid sequences that can be surveyed in a random population is frequently insufficient to include sequences mediating the desired function. However, if the population is biased such that all members contain at least some of the desired amino acid sequence, fewer additional sequence contributions are necessary. A method used to construct repeating polypeptide populations facilitates an interative approach to the search for proteins displaying novel properties (Brown, 1997). It can be seen in Figure 1 that part of the repeating unit is derived from random nucleotides and part is derived from predetermined,

Abbreviations used: .

E-mail address of the corresponding author: stanley@biobase.dk

0022-2836/00/030725–11 $35.00/0

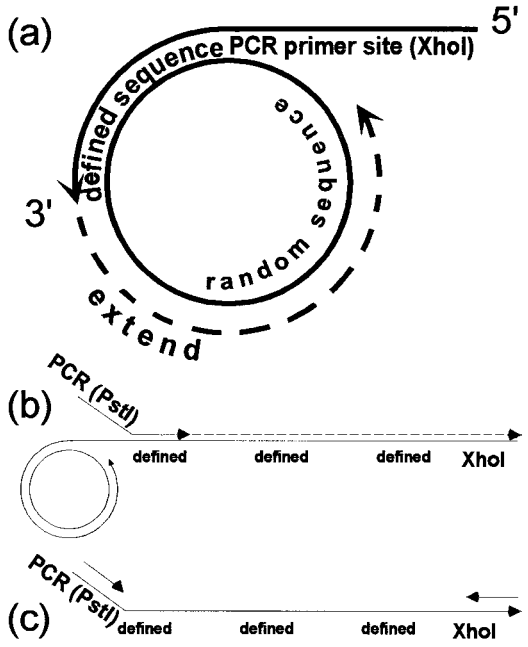

Figure 1. Contruction of libraries. Circular single-stranded oligonucleotides containing 50 or 45 random nucleotides and 13 or 18 nucleotides of defined sequence (see Materials and Methods and Figure 2) were circularized to generate the circular template in (a) the circular template was annealed with an oligonucleotide whose 3′ portion was complementary to the defined nucleotides of the circular template and whose 5′ portion included an *Xho*I recognition site within a primer site for later PCR amplification. The linear oligonucleotide was extended around the circular template many times to generate the repeating oligonucleotide in (b) An oligonucleotide whose 5′ portion included a *Pst*I recognition site within a primer site for later PCR amplification was annealed to the defined nucleotides in the repeating oligonucleotide and extended by DNA polymerase. (c) The repeating oligonucleotide was amplified by PCR. The resulting double-stranded repeating oligonucleotide was digested with *Pst*I and *Xho*I, and cloned (see Materials and Methods).

defined nucleotides. The sequence of the defined nucleotides can be designed to encode amino acid sequences known to display traits desirable in a particular search.

We have instituted an iterative genetic strategy and identified gold-binding proteins that altered the rate of gold colloid appearance. The proteins that accelerated the rate of colloid appearance altered the morphology of the crystals. Analysis of these proteins reveals that two traits participate in the alteraction of crystal shape. First, they contain a catalytic function that appears to act by acid catalysis. Second, they adhere to gold. The role of adhesion is probably to increase the concentration of the catalytic function at the surface of the growing crystal.

Results

Second-generation libraries

Previous analyses indicated that the binding properties of partially random repeating polypeptides is influenced by the defined sequence portion of the template oligonucleotide (Brown, 1997; and see Figure 1). Two populations were prepared (see Materials and Methods) in which the defined sequence was likely to contribute to gold-binding (Figure 2). One population had a defined sequence encoding KTQATS, part of a gold-binding repeat unit found previously (Brown, 1997). The other population had a defined sequence encoding SKTS, an aggregate of the most frequent dipeptides found among gold-binding repeating polypeptides (Brown, 1997; and data not shown). The repeating polypeptides were expressed on the outer surface of *Escherichia coli* from oligonucleotides inserted in the gene coding for the λ-receptor, *lamB* (reviewed by Newton *et al.*, 1996). Populations of bacteria harboring the modified *lamB* libraries, derived from KTQATS and SKTS-encoding templates, contained 10^6 and 5×10^5 members, respectively. Each member is derived from a different template oligonucleotide, thus expressing a repeating polypeptide with a different amino acid sequence. Individual clones contained from three to approximately 20 repeats of the inserted oligonucleotide.

Library A: lq(sktsX$_{17}$)$_{3-20}$sktsle
Library B: lqt(qatsX$_{15}$kt)$_{3-20}$qatsle

Accelerators of crystal appearance
RP1: lq(sktsLGCQKPLYMGREMRMLT)$_2$-
(sktsLGQSGASLQGSEKLTNG)$_5$sktsle
RP2: lqt(qatsEKLVRGMEGASLHPAkt)$_9$qatsle

Alignment of accelerators
RP1: LGQSGASLQGSEKLTNGsktsLGQSGASLQGSEKLTNG
RP2: qatsEKLVRG------MEGASLHPAkt

Retarders of crystal appearance
RP4: lq(sktsTNNFGGMMPGGDESTKI)$_{17}$sktsle
RP5: lqt(qatsEMQRQMGIRVGPEQDkt)$_{11}$qatsle

Other repeating polypeptides
RP6: lqt(qatsGSERMGHQSGTVHPGkt)$_7$qatsle
RP1′: lqt(sktsLGQSGASLQGSEKLTNG)$_5$qatsle
RP6/1′: lqt(qatsGSERMGHQSGTVHPGkt)$_7$qatsld-
ggggsmqt(sktsLGQSGASLQGSEKLTNG)$_5$sktsle

Figure 2. Amino acid sequences of repeating polypeptides. The format of the libraries (see Materials and Methods) and the inferred amino acid sequence of the isolated mutants are shown. Amino acids (X) derived from the random portions of the template oligonucleotides are displayed in upper case. The defined amino acids are displayed in lower case. The two tetrapeptides found in both accelerators are underlined. The amino acids encoded by the accelerators are shown aligned as repeating polypeptides.

Mutant search

The search for mutants that modulated the morphology of gold crystals was conducted in two steps. The first step assumed that proteins that modulate crystal morphology will adhere to metallic gold. The second step assumed that an altered crystal morphology would be accompanied by an altered rate of colloid formation. Candidates were first enriched for their ability to adhere to metallic gold (see Materials and Methods). After each cycle of enrichement, the complexity of the population was examined by measuring the size-distribution of the inserted oligonucleotides (Brown, 1992). After five cycles of enrichment, the complexity of the population was greatly reduced by this assay. For the second step, the inserted repeating oligonucleotides were transferred from the *lamB* gene of the enriched population to the *phoA* gene, encoding alkaline phosphatase (see Materials and Methods). This allowed us to examine the influence of the repeating polypeptides as part of a soluble protein. The resulting alkaline phosphatases were examined individually for their influence on the rate of gold colloid formation by measuring the time from addition of reducing agent to the first appearance of pink color (see Materials and Methods). In this manner, 50 mutants were tested and five were identified that altered the time necessary for the color change compared with control shock fluid from the vector-bearing strain. Three mutants reduced the time necessary for color appearance and two mutants increased the time necessary for color appearance. We designated these repeating polypeptide-alkaline phosphatase hybrid proteins RP1 through RP5.

Sequence analysis

DNA sequence analysis showed two of the mutants that reduced the time of colloid appearance, RP1 and RP3, were siblings and only one of these, RP1, encoded by pSB3204, was examined further. The other mutant that reduced the time of colloid appearance, RP2, was encoded by pSB3218. The two mutants that retarded colloid appearance, RP4 and RP5, were encoded by pSB320 and pSB3243, respectively. The deduced amino acid sequences of the repeating polypeptides are shown in Figure 2.

The sequences of the clones encoding the accelerators of gold colloid appearance show the following features. RP1 is encoded by a clone derived from two templates. This event probably occurred during the polymerase chain reaction (PCR) step in the construction of the initial libraries. The C-terminal repeating peptides have sequence similarity with the other accelerator of colloid appearance, RP2. Both contain two tetrapeptides, SEKL and GASL. The high degree of sequence similarity leads to two conclusions. First, both repeating polypeptides are likely to influence gold colloid appearance by the same mechanism. Second, few possible amino acid sequences are likely to accelerate the appearance of gold colloids. The alignment of the two tetrapeptides in the context of the repeating polypeptide is shown in Figure 2. No obvious sequence similarity is present between RP4 and RP5, the two mutants that retard the rate of colloid appearance.

Gold crystals formed by accelerators

If the repeating polypeptides accelerate colloid appearance by altering the direction of crystal growth, the resulting crystals would have an altered morphology. Since gold particles composed of as few as 50 atoms have the crystalline face-centered cubic (fcc) structure of bulk gold (Balerna *et al.*, 1985), it is likely the initial colloids formed were composed of crystalline particles. RP1, RP2 and control alkaline phosphatase encoded by the vector were prepared in parallel by method A (see Materials and Methods). Gold particles were formed in the presence of the preparations and examined by transmission electron microscopy (Figure 3). The formation of large, thin, hexagonal crystals were stimulated by RP1 and RP2. The continuous pairs of lines seen across the faces of the flat crystals are due to bending of the thin crystals (Williams & Carter, 1996). In addition to the large, thin, hexagonal crystals, smaller ''spherical'' crystals were formed. Gold crystals formed in the presence of RP1 or RP2 were aggregated. Occasionally, small, flat, irregular crystals were formed in the presence of alkaline phosphatase lacking a repeating polypeptide (Figure 3(e)). Large, thin crystals were not seen among crystals grown in the presence of vector-encoded alkaline phosphatase. In addition, the large, thin crystals were not observed in gold crystallized in the absence of added protein, in the presence of another protein, bovine serum albumin, or in the presence RP4 or RP5.

RP1, RP2 and vector-encoded alkaline phosphatase were each prepared twice from independent colonies and the crystallization results were indistinguishable between the two sets of experiments. The only component that varied between these preparations was the repeating polypeptide. Thus, the entity inducing the formation of the large, thin crystals is contained, at least in part, by the repeating polypeptide portions RP1 and RP2. The molar ratio of repeating polypeptide to $AuCl_3$ was approximately 1:300 in these experiments.

The shape of the large, thin crystals provides an explanation for the acceleration of crystal appearance. The large face on the protein-induced crystals is (111), verified by electron diffraction (data not shown). The {111} family of faces (Figure 4) are those with the fewest number of broken bonds per atom and the lowest surface energy. That is, bringing in another gold atom from the solution above the gold-solvent interface to the growing crystal is least energetically favored at the {111} faces. Since more energy is released by adding a gold atom to

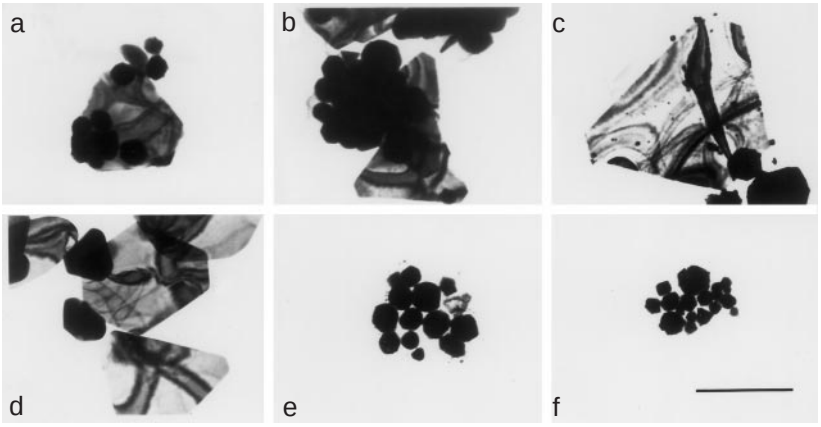

Figure 3. Gold crystals formed by accelerators of crystallization. Crystallizations were performed with approximately 40 μg/ml alkaline phosphatase purified by method A (Materials and Methods). Crystallizations containing the supplements indicated below were incubated at room temperature and prepared for transmission electron microscopy (Materials and Methods). Crystallizations containing protein supplements were incubated 1 h and crystallizations lacking protein supplements were incubated 30 min. (a) RP2, (b) RP1, (c) 200 μM $AuCl_3$, 200 μM ascorbic acid and no other solutes, (d) crystals prepared from a boiling solution of 200 μM $AuCl_3$ and 500 μM citric acid and no other solutes, (e) vector-encoded (pSB2991) alkaline phosphatase, (f) 200 μM $AuCl_3$, 200 μM potassium ascorbate pH 7, 10 mM potassium phosphate pH 7 and no other solutes. All images are presented at the same magnification. The bar in panel F represents 300 nm.

faces other than {111}, crystal growth can be accelerated by biasing accretion onto a face other than {111}, thus increasing the area of the {111} faces. If accretion on all eight {111} faces were equally biased by the proteins, the process would be self-limiting as the {111} faces expand to form an octahedron (Figure 4). If accretion on only two of the {111} faces was affected by the proteins, the crystals could continue to expand by atoms accreting onto more energetically favorable faces. This would result in the formation of thin plates and can account for the phenotype of accelerated appearance of pink color that was the basis of our genetic screen.

Effects of pH

Crystals similar to those induced by mutant RP1 and RP2 have been reported (Turkevich *et al.*, 1951), formed by reducing $AuCl_3$ with boiling citric acid. Large, thin, pseudo-hexagonal crystals formed in boiling citric acid (Figure 3) are similar to those induced by the repeating polypeptides at neutral pH and room temperature. Similar crystals have been observed under a variety of acidic conditions if crystal growth is slow (Southam & Beveridge, 1994; Mayer & Antonietti, 1998; Flores *et al.*, 1998). Similarly shaped crystals of another metal, silver, have been observed in *Pseudomonas* sp. isolated from a silver mine, but no mechanism for their formation was investigated (Klaus *et al.*, 1999).

The observation that crystals formed from RP1 and RP2 at room temperature and neutral pH are similar to those formed from boiling acid raises the question of which factor the repeating polypeptides are mimicking, the acidic conditions or the high temperature. In order to identify the relevant factor, crystals were formed by reduction with ascorbate in neutral and acidic conditions at room temperature. The gold crystals formed from acidic conditions appear similar to the flat crystals formed in the presence of the repeating polypeptides and the gold crystals formed at pH 7 appear similar to the crystals formed in the presence of vector-encoded alkaline phosphatase (Figure 3).

Enzymes often catalyze reactions by general acid or base catalysis (Fersht, 1998). We tested whether such a mechanism could alter the crystal shape of gold by varying the pH and buffer concentrations. At pH 4, 4 % (91 of 2581) of the crystals were thin and flat, and 1 % (21 of 1724) were thin and flat at pH 5. We observed no thin, flat crystals at pH 6. The fraction of crystals that were thin and flat varied only with pH, not with the concentration of sodium acetate when this varied from 0 to 20 mM. Similarly, the rate of color appearance varied only with pH, not with the presence or absence of 10 mM sodium acetate. Thus, the alteration of crystal shape by the repeating polypeptides is likely to be by regulation of the proton concentration, i.e. pH, rather than by contributing an acid group, i.e. general acid catalysis.

Gold crystals formed by retarders

RP4, RP5 and vector-encoded alkaline phosphatase were purified by method A (see Materials and Methods). The gold crystals formed in the presence of RP4 or RP5 were similar to those formed in the presence of vector-encoded alkaline phosphatase, except no flat, thin crystals of any size were observed (data not shown). We propose no mechanism for the retardation of colloid appearance mediated by RP4 or RP5.

Face-specific binding

Although the most likely mechanism by which RP1 and RP2 alter crystal morphology is by acid catalysis, they could act by preferentially obscuring {111} faces and thus biasing accretion to the other crystallographic faces. This mechanism has been proposed for protein-mediated control of calcium carbonate crystal growth, although face-specific binding was not measured (DeOliviers & Laursen, 1997). If that was the mechanism here, the products of RP1 and RP2 should preferentially bind to {111} faces compared to a gold-binding protein that did not induce the formation of similar crystals. We compared the binding of three repeating polypeptides to gold that was predominantly displaying {111} faces and to isometric crystals of gold. The different gold samples were prepared and the binding of radiolabeled repeating polypeptide-alkaline phosphatase hybrid proteins was measured (see Materials and Methods). The results shown in Table 1 indicate that RP1 and RP2 had no higher preference for binding to gold reduced from acid conditions than RP4. Thus, the accelerators of crystallization did not preferentially bind to {111} faces. The experiments summarized in Table 1 were conducted at sub-saturating concentrations of hybrid proteins. As expected, as saturating concentrations all three hybrid proteins were similar in their relative binding to the two preparations of gold (data not shown). The absence of face-specific binding is consistent with a model where the function of the gold-binding trait is to elevate the concentration of the catalytic function at the surface of the growing gold crystal.

Is RP2 incorporated into the gold crystal?

When RP2 altered the crystal morphology of gold, did it associate only with the surface of the growing gold crystal or did it incorporate within the crystal? That is, are the gold crystals formed in the presence of RP2 pure gold or a gold/protein composite?

If the repeating polypeptide associated with the crystal surface and the association was dependent on the folded structure of the repeating polypeptide, then unfolding the polypeptide may release it from the gold. However, if the repeating polypeptide became integrated into the gold crystal during crystal growth, for example as a guest molecule, then detergents that unfold proteins would not release the incorporated repeating polypeptide. Similarly, if the repeating polypeptide was covalently associated with the gold crystal, it would not be released by detergents. Thus, detergent-mediated release of RP2 from the gold crystals formed in its presence would occur only if the protein was non-covalently associated with the outer surface of the gold crystal.

We measured the detergent-resistant binding of RP2 and alkaline phosphatase encoded by the vector, pSB2991 (see Materials and Methods). In the experiment (see Table 2), the vector-encoded alkaline phosphatase preparation contained 19 ng of alkaline phosphatase and 26,200 cpm of ^{35}S, of which 57 % was as alkaline phosphatase. The RP2 preparation contained 24 ng RP2 and 19,200 cpm of ^{35}S, of which 55 % was as RP2. In our calculations, we assumed that all of the radioactivity remaining associated with the gold was due to alkaline phosphatase, that is, radioactivity of the repeating polypeptide portion, if buried within the gold crystal, may not be detected by scintillation counting. This is the most conservative estimate of residual molar binding. We also assumed that all of the added $AuCl_3$ was converted to gold metal. Based on these assumptions, we calculated the molar binding of the vector-encoded and RP2 alkaline phosphatases. The amount of RP2 that remains associated with gold formed in its presence is entirely accounted for by the amount that failed to disassociate from pre-formed gold and the amount of vector-encoded alkaline phosphatase that was trapped by gold formed in its presence. We conducted this experiment three times with two different preparations. In the other two experiments, we found the maximum amount of RP2 retained by gold formed in its presence that could not be accounted for by non-specific binding represented 0 and 0.2 fmol of repeating polypeptide per nanomole of gold. Thus, very little protein remained associated with gold, ruling out its excessive incorporation within the gold crystal during crystal growth.

Table 1. Face-specific binding

Shockate	Gold	Shockate (μl/nmol gold)	Ratio acid/neutral
RP1	Acid	0.014	0.48
	Neutral	0.029	
RP2	Acid	0.019	0.39
	Neutral	0.049	
RP4	Acid	0.018	0.53
	Neutral	0.034	

Binding to predominantly {111} (acid) and isometric (neutral) gold crystals were measured (Materials and Methods). Binding is reported as the volume of shock fluid containing the retained amount of hybrid protein. The ratio of binding to the two forms of gold crystals is reported.

Table 2. Incorporation of proteins

Alkaline phosphatase	Gold	cpm retained	Alkaline phosphatase (fmol/nmol gold)
Vector	Preformed	29	0.026
	$AuCl_3$	110	0.15
RP2	Preformed	318	0.35
	$AuCl_3$	299	0.50

Incorporation of proteins. Each reaction received [^{35}S]methionine-labeled alkaline phosphatase preparations and the indicated form of gold. Radioactivity remaining with the gold is reported. Molar binding is described in the text.

Genetic analysis of flat-crystal mediators

The repeating oligonucleotide of the RP1-encoding plasmid, pSB3204, was derived from two templates such that the five C-terminal peptides were similar to the other accelerator of crystal appearance, RP2, and the two N-terminal peptides were not. We constructed a clone producing a truncated RP1 missing the two N-terminal peptides (see Materials and Methods). We designated the truncated product RP1′. We purified RP1 and RP1′ by method B (see Materials and Methods) and found that RP1′ induced the appearance of large, thin crystals at a much lower frequency than RP1 (data not shown). The two N-terminal repeats of RP1 probably augment gold-binding, since RP1′ had reduced avidity for metallic gold compared with RP1 (data not shown). This suggests the ability to modify crystal morphology requires two functions, binding to gold and the function mediated by the SEKL and GASL-containing repeats.

We tested the role of gold-binding in the following manner. The gold-binding repeating polypeptide RP6, encoded by pSB3246, was identified in the initial analysis as one that did not alter the rate of crystal appearance. We found that RP6 purified by method B (see Materials and Methods) did not induce the appearance of flat crystals (data not shown). We generated a tripartite protein, RP6/1′, that contained the seven repeats of RP6 followed by the five repeats of RP1′ and alkaline phosphatase. RP6/1′ purified by method C (see Materials and Methods) efficiently generated large, thin crystals (data not shown). In addition, RP6/1′ induces the appearance of another class of gold crystals. These crystals also have the (111) face as large face as determined by electron diffraction, but are exceptionally thin with irregular edges (Figure 5). The moiré pattern shows where two flat crystals are overlapping and slightly rotated relative to each other. Similar rounded edges can be seen among crystals formed from boiling citric acid. Although we have not observed the exceptionally thin crystals formed in the absence RP6/1′, their poor contrast in transmission electron microscopy renders them difficult to detect. None-the-less, their frequent occurrence in the presence of RP6/1′ shows crystal morphology can be readily modified by the products of simple genetic transactions.

Discussion

Several conclusions can be reached from the experiments described above. We have recovered proteins, in this case repeating polypeptides, that modulate crystal morphology. The protein-mediated modulation of crystal morphology is not limited to those crystals found in biological materials. The recovered proteins display three properties expected of enzymes. First, they act catalytically and are not incorporated into the product. Second, they appear to act by a mechanism of acid catalysis. Third, the two repeating polypeptides that mediate the same process display sequence similarity with each other.

Catalytic nature of activity

The repeating polypeptides are released from the crystals formed in their presence by conditions that lead to protein denaturation (Laemmli, 1970). This shows they are neither covalently bound to the

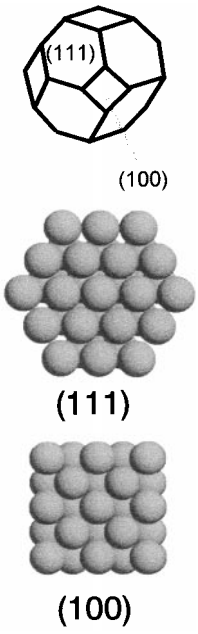

Figure 4. Atomic configuration on crystallographic planes. The top panel depicts a cuboctahedral crystal of gold. There are eight {111} and six {100} facets. The lower panels show atomic configuration on the (111) and (100) crystallographic planes.

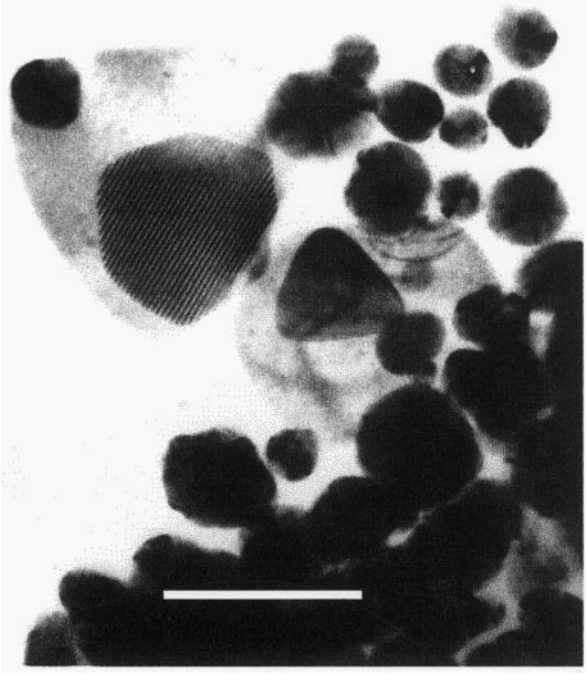

Figure 5. Genetic reconstitution of crystallizing polypeptide. Crystallization was performed with approximately 0.5 μM RP6/1′ (see Materials and Methods). Crystallization reaction was incubated at room temperature for 30 minutes and prepared for transmission electron microscopy (see Materials and Methods). The scale bar represents 100 nm.

surface nor incorporated into the gold crystal. Since the repeating polypeptide of RP2 contains no cysteine residue, the reducing agent present during protein denaturation cannot act through any thiol group in the repeating polypeptide. If backgrounds are subtracted for binding to preformed crystals and binding by the vector-encoded alkaline phosphatase, no RP2 remains associated with the crystals formed in its presence. Even without subtracting backgrounds, the residual protein is very low.

Since the protein is not incorporated into the gold crystal, it is not forming a composite. In addition, the protein is not acting to obscure the large, flat faces, since it does not preferentially bind to those faces. We favor the explanation that the protein is acting to bias accretion on the thin edges of the flat crystals. Since crystals of the same shape are formed from acidic conditions, the simplest model for the action of the proteins is they alter the chemical environment, emulating acidic conditions. The role of acids in control of gold crystal morphology appears to be through the control of pH rather than as general acids. We propose the repeating polypeptides are acting similarly, by controlling the local pH, although general acid catalysis is the common mechanism among enzymatic reactions (Fersht, 1998).

Shape of the gold crystals

The crystal structure of gold is close-packed, fcc. The equilibrium shape of a free crystal is the shape that minimizes the total surface energy for a fixed volume. For crystals with facets, facet area is inversely related to the surface energy of that facet. That is, faces of lower surface energy form larger facets (Porter & Easterling, 1992). Many metals and a variety of other materials with cubic structure have an equilibrium shape dominated by {111} faces and {100} faces, indicating that these faces have the lowest energies. Most fcc metals, including gold, have cuboctahedral equilibrium shape (Figure 4) with {111} facets that have a slightly lower surface energy than the {100} facets, reflected as {111} facets having a slightly larger area than {100} facets. Due to symmetry, this type of morphology should always sustain crystals with isometric shape even if they are multiply twinned, i.e. containing boundaries of paired crystals on all four types of {111} planes. A flat gold crystal with one pair of large (111) faces must be a non-equilibrium shape and its shape must be mediated by a process that prevents addition of atoms to this pair of faces as rapidly as to other faces. This can occur either by slowing their growth-rate or by increasing the speed of the others growth-rate. The kinetic argument presented in Results reconciles the observation of thermodynamically unfavored crystal shapes with an accelerated rate of appearance. The proteins bias crystal growth in a manner that allows continued accretion onto energetically favorable faces.

We have identified the large, flat face of the protein-induced crystals as the (111) face. However, we were unable to identify the nature of the edges of the large, flat crystals. An intriguing possibility is that the large, flat crystals contain an internal twin boundary parallel with large, flat faces. In this case, the edges of the plate will contain notches (re-entrant facets). The re-entrant facets have a slightly higher energy than the flat {111} facets (Cleveland *et al*., 1997) and will thus provide sites for extended growth parallel with the large, flat {111} facets. There is a precedence for twinned crystals of this nature that suggests a model for their generation. Clusters are exceptionally small crystals that behave like molecules of metals. Cleveland *et al*. (1997) have solved the structures of larger gold clusters. They find that clusters containing 225 and 459 gold atoms have one internal twin boundary and re-entrant edges. If the proteins adhere to these nuclei, they may lower the surface energy of the {111} faces and hence provide accelerated growth of the lateral, re-entrant edges. Large gold nuclei and crystals will develop multiple twins (Figure 5; reviewed by Marks, 1994). Once the crystals become multiply twinned, the protein will no longer be able to favor expansion of one pair of (111) faces. Thus, the mixture of

crystal shapes would result from competing processes.

Genetic control of crystal shape

Gold-binding was a requirement in the isolation of the repeating polypeptides characterized in this study. Our ability to separate the gold-binding from the catalytic function in RP1 allowed us to examine the role of binding to metallic gold in crystal formation. We found that removal of the gold-binding repeats of RP1 greatly reduced the production of large, thin crystals and restoration of heterologous gold-binding repeats restored efficient formation of large, thin crystals. Hence, the repeating polypeptide-mediated crystal formation was greatly enhanced by binding to gold. This effect was probaly due to an increase in the local concentration of the repeating polypeptide at the surface of the growing crystal. This hypothesis is supported by the lack of face-specific binding by RP2. That is, bringing the catalytic function to the surface of the growing crystal increased its activity. Furthermore, since the growing gold crystal is one of the substrates in crystal growth, one should expect binding of one of the substrates to influence the reaction. What was surprising is the degree the reaction products appeared altered with a change in gold-binding domain. That is, changes in crystal-binding of a protein that controls crystal shape lead to new crystal morphologies.

An evolutionary model

Biogenesis of the minerals present in hard tissue has been a subject of extensive study (Addadi & Weiner, 1985; Mann, 1988; Simkiss & Wilber, 1989; Falini *et al*., 1996; Belcher *et al*., 1996; Fincham *et al*., 1999). In these cases, crystal morphology is influenced by the stereochemical properties of the solvent (Mann *et al*., 1990; Weissbuch *et al*., 1991). Thus, both the formation and continued growth of a crystal may be subject to the surrounding chemical environment. In light of this, we wish to point out some surprising similarities between our observations and the structure of biological hard tissue, and present a speculative evolutionary hypothesis. In a number of hard tissues, the inorganic crystallites, like the flat gold crystals induced by the repeating polypeptides, have as their broadest faces those of highest ionic or atomic occupancy. Also, the biomineral crystallites have the faces of lowest occupancy as the most rapidly advancing faces. For example, twinned aragonitic crystallites in mother-of-pearl of mollusc shells result from the accelerated accretion on {110} faces, the planes of lowest occupancy (Sarikaya *et al*., 1995). Similarly, in mammalian dentin and bone, flat hydroxyapatite crystallites have {0001} faces as the broadest faces with an aspect ration of 15:1 and the {0001} faces of hydroxyapatite have 50% greater ion occupancy than the faces of rapid accretion, the $\{\bar{2}110\}$ faces (Simmer & Fincham, 1995). Thus, the shape of crystals in hard tissue, although thermodynamically poorly favored, is kinetically highly favored. This is the same argument that explained our observations of gold crystal morphology influenced by RP1 and RP2. The kinetic argument raises the possibility that the initial evolutionary advantage that fixed the crystal-forming processes may have been rapid crystal growth. That is, the ancestral organism benefited by generating the crystals most rapidly. If so, the elaborate architectures seen in hard tissues of modern organisms reflect the initially selected crystallographic forms.

Conclusions

In summary, the results of our experiments suggest that features common among enzymes can modify the crystallization of inorganic material. We suggest that such mechanisms be considered in the formation of the crystalline phases of hard tissue. Furthermore, we propose that the genetic approach instituted is a general one that should be applicable to other inorganic materials. If this is the case, such an approach may lead to new understanding of the mechanisms of protein function and provide insights in fields of chemistry not yet influenced by genetic analysis.

Materials and Methods

Strains, plasmids, media and buffers

The *lamB* expression plasmid pSB2267 and the *phoA* expression plasmid pSB2991 and *E. coli* strains S2157 and S2188 have been described (Brown, 1997). Transformants were grown in YT medium (Miller, 1972) supplemented with 25 μg/ml chloramphenicol for pSB2267-derivatives or 100 μg/ml ampicillin for pSB2991-derivatives. Radiolabeling with L-[^{35}S]methionine was conducted in M63 salts (Miller, 1972) supplemented with 1 μg/ml thiamine, 0.4% (w/v) glucose, 40 μg/ml proline and 100 μg/ml ampicillin. PKT buffer (10 mM potassium phosphate (pH 7.0), 0.1 M KCl, 1% (v/v) Triton X-100; Brown, 1997), was used for *in vitro* binding assays.

Libraries and DNA-manipulations

Repeating oligonucleotides were prepared by the rolling circle method (Fire & Xu, 1995; Liu *et al*., 1996; Lizardi *et al*., 1998) as described (Brown, 1997) and depicted in Figure 1. Templates were 5′ ACCAGC$(NNS)_{16}$NNCTCCAAG 3′ for the SKTS library, and 5′ GCGACCAGC$(NNS)_{15}$AAGACTCAG 3′ for the KTQATS library. N denotes a mix of all four nucleotides and S denotes a mix of G and C. *Xho*I recognition site-containing rolling circle primers were 5′ CCAGTTGCTCTCGAGGCTGGTCTTGGA 3′ and 5′ CCAGTTGCTCTCGAGGCTGGTCGCCTGAGTCTT 3′. *Pst*I recognition site-containing primers for second strand synthesis were 5′ GGTTCACAGGCTTGGTCTGCAGTCCAAGACCAGC 3′ and 5′ GGTTCACAGGCTTGGTCTGCAGACTCAGGCGACCAGC 3′. PCR primers were 5′ GGTTCACAGGCTTGGTCTGCAG 3′ and 5′ CCAGTTGCTC-

TCGAGGCTGGT 3′. Double-stranded repeating oligonucleotides were cleaved with *Pst*I and *Xho*I, cloned in pSB2267 and transformed into S2188.

Plasmid DNA from the enriched populations was isolated, the repeating oligonucleotides recloned by *PstI and Xho*I into pSB2991, and transformed into S2157. DNA sequences of p2991-derivatives were determined using cycle-sequencing, and primers 5′ TTCCCCCTGATAAGACGCGAC 3′ and 5′CGCAGAGCGGCAGTCTGATC 3′. The two 5′ repeats of pSB3204 were removed by PCR using 5′ GGCAGGGAGATGGCGCTGCAGACCTCCAAG 3′ to introduce a *Pst*I recognition site between the second and third repeat to produce pSB3272, encoding RP1′. The linker used to generate pSB3278, encoding RP6/1′, was from a *Sal*I-*Nsi*I fragment encoding the single-chain antibody linker, Gly-Gly-Gly-Gly-Ser (Huston *et al*., 1988) of sequence 5′ GTCGACGGTGGTGGCGGTTCTATGCAT 3′.

Enrichment procedure

Populations were enriched for those bacteria adhering to metallic gold in a manner similar to that described (Brown, 1997). Cultures of the populations were established in YT broth supplemented with 25 μg/ml chloramphenicol at 30 °C and expression of the λ-receptor induced for 20 minutes with 0.1 mM IPTG. Induced cultures were diluted into 90 % (v/v) Percol in 10 mM potassium phosphate (pH 7.0), 0.1 M KCl and HF-washed gold powder (Brown, 1997) was added to 1 mg/ml. Adhesion was permitted for 20 minutes at room temperature and the gold with adhering bacteria recovered by centrifugation. The supernatant was discarded and the gold resuspended with YT broth and trypsin, Tris-HCl (pH 8.0) and $CaCl_2$ added to final concentrations of 1 mg/ml, 20 mM and 2 mM, respectively. After 30 minutes at 37 °C, all bacteria and gold were recovered by centrifugation and resuspended with the above Percol solution. Gold was removed by centrifugation and the supernatant with released bacteria diluted into YT broth supplemented with 25 μg/ml chloramphenicol and grown overnight. The enrichment procedure was repeated the next day.

Gold crystallization assay

The assay used to search for mutants was conducted in PKT buffer containing 250 μM $AuCl_3$ neutralized with KOH and osmotic shock fluid (Ducancel *et al*., 1989) from IPTG-induced transformants containing approximately 1 μg of hybrid alkaline phosphatase. Sodium ascorbate (Stathis & Fabrikanos, 1958) was added in varying amounts to bring the final concentration of ascorbate to 50-200 μM and the total volume to 1 ml. Shock fluid from each mutant was tested with several concentrations of ascorbate. Reactions were incubated at room temperature and time to first appearance of pink color noted. Gold crystallization in the pH-curve experiments was conducted as above but without PKT buffer. Gold crystallization in the presence of alkaline phosphatases for electron microscopy was conducted as above but with $AuCl_3$ at 200 μM and potassium ascorbate at 400 μM.

Preparation of alkaline phosphatase

Cultures of S2157 harboring the vector pSB2991 or one of the mutant plasmids were established in YT broth supplemented with 100 μg/ml ampicillin at 34 °C. Fresh, overnight colonies were used, since S2157 harboring pSB3204 or pSB3218 were sensitive to storage on agar. At an absorbance at 600 nm of 0.7, the expression was induced with 1 mM IPTG for 20 minutes. Cells were recovered by centrifugation at 4 °C, and osmotic shock fluid prepared (Ducancel *et al*., 1989). Alkaline phosphatase was purified by the shock fluid by one of three methods. In method A, the shock fluid was passed over DEAE-Sephacel in 20 mM Tris-HCl (pH 8.0). The columns were washed with 20 mM Tris-HCl (pH 8.0). Partially purified alkaline phoshatase was eluted with 20 mM Tris-HCl, made to 0.1 M NaCl, and dialyzed into 10 mM potassium phosphate (pH 7.0), 0.1 M KCl. Hybrid and vector-encoded alkaline phosphatase in these preparations represented greater than 50 % of total protein as determined by gel electrophoresis and staining with Coomassie brilliant blue. Equal volumes of the dialysates were used in all experiments with partially purified alkaline phosphatases prepared by method A. Radiolabled RP2 and alkaline phosphatase encoded by pSB2991 were prepared similarly but from M63 salts medium. More highly purified RP1, RP1′ and RP6 were prepared by method B. In method B, the shock fluid was passed over DEAE-Sephacel in 20 mM Tris-HCl (pH 8.0) and the columns washed with 20 mM Tris-HCl (pH 8.0). The hybrid protein was eluted from DEAE-Sephacel with 20 mM Tris-HCl, made to 50 mM NaCl, and hybrid protein-containing fractions were pooled and chromatographed over Sephadex G-150 in 10 mM potassium phosphate (pH 7), 0.1 M KCl. RP6/1′ failed to bind to DEAE-Sephacel and was purified by method C. In method C, the shock fluid was made to 10 mM NaCl and passed over DEAE-Sephacel equilibrated in 20 mM Tris-HCl (pH 8.0). The eluate was diluted with four volumes 10 mM sodium phosphate (pH 7), 10 mM NaCl and passed over carboxymethyl cellulose (Whatman CM-52) equilibrated with 10 mM sodium phosphate (pH 7). The column was washed with 10 mM sodium phosphate (pH 7), 10 mM NaCl, and RP6/1′ was eluted with 50 mM sodium phosphate (pH 7), 0.2 M NaCl. RP6/1′-containing fractions were pooled and chromatographed over Sephadex G-150 in 10 mM potassium phosphate (pH 7), 0.1 M Kcl. The concentrations of hybrid protein prepared by methods B and C were determined by measuring absorbance at 205 nm and comparing the absorbance with that measured for bovine serum albumin standards. Hybrid proteins prepared by methods B and C were greater than 85 % of total protein as determined by gel electrophoresis and staining with Coomassie brilliant blue, and were used at 0.5 μM in gold crystallizations for transmission electron microscopy.

Gold-binding measurements

Cultures were radiolabeled and osmotic shock fluid prepared. Acid gold was prepared from a boiling solution of 200 μM $AuCl_3$ and 500 μM citric acid and no other solutes; and neutral gold was prepared from 200 μM $AuCl_3$, 200 μM potassium ascorbate (pH 7.0), 10 mM potassium phosphate (pH 7.0) and no other solutes, and both were dialyzed against water. Gold and shock fluids were diluted in PKT before mixing. Shock fluid was used at subsaturating concentrations. The amount of gold in a final reaction volume of 1 ml represented from 2-32 nmol $AuCl_3$. Proteins were allowed

to adsorb 40 minutes at room temperature. Gold with any adhering protein was collected at 9800 *g* for five minutes at room temperature, resuspended with SDS sample buffer (Laemmli, 1970), boiled and electrophoresed on 8% (w/v) polyacrylamide gels (Laemmli, 1970). Adhesion to HF-washed gold powder was performed as described (Brown, 1997). Radioactivity in RP1, RP2 and RP4 was quantified by phosphor-imaging.

Release of proteins from gold

Cultures were radiolabeled with [^{35}S]methionine and alkaline phosphatases prepared by method A. The amount of alkaline phosphatase was determined by electrophoresis on 8% polyacrylamide gels (Laemmli, 1970), staining with Coomassie brilliant blue and comparison with bovine serum albumin. The fraction of total radioactivity present in vector or hybrid alkaline phosphatase was determined by phosphor-imaging. Preformed colloidal gold was prepared as for neutral gold and dialyzed against water. Reaction volumes of 0.1 ml contained either colloidal gold derived from 30 nmol of $AuCl_3$, or 20 nmol of $AuCl_3$ and 50 nmol of potassium ascorbate in PKT buffer. Protein was added prior to the addition of gold. Ascorbate was added last. Reactions were incubated at room temperature in the dark for one hour. Reactions were diluted with 0.9 ml of 1% (w/v) SDS in 10 mM Tris-HCl (pH 7.8) and gold collected at 9800 *g* for ten minutes. The supernatant was discarded and gold resuspended with 1 ml of 1% SDS, 10 mM DTT, 10 mM Tris-HCl (pH 7.8) and incubated at 90°C for five minutes. The gold was collected as described above and the supernatant discarded. The gold was washed with 1 ml of 1% SDS, 10 mM Tris-HCl (pH 7.8) and 0.18 ml of water. The samples were dried at 60°C and radioactivity determined by scintillation counting.

Electron microscopy

Approximately 1 µl aliquots of the gold crystallization reactions were suspended onto a thin carbon film attached to a Cu grid. The samples were dried in a desiccator at room temperature in still air. Transmission electron microscopy was performed with a single-tilt holder using a Philips EM400T microscope at 100 kV or a Philips CM20 at 200 kV.

Sequence accession codes

Sequences have been deposited in Genbank with accession numbers AF247169-AF247176.

Acknowledgments

We thank Beth Traxler for the hospitality of her laboratory. We thank Robert DeLotto, Harvey Eisen, Bart Kahr, Steve Lory, Steen Pedersen, Karen Skriver, Geneviève Thon and B. Traxler for comments on the manuscript. This work was supported by Danish Research Councils and the U.S. Army Research Office.

References

Addadi, L. & Weiner, S. (1985). Interactions between acidic proteins and crystals: stereochemical requirements in biomineralization. *Proc. Natl Acad. Sci. USA,* **82**, 4110-4114.

Balerna, A., Bernieri, E., Picozzi, P., Reale, A., Santucci, S., Burattini, E. & Mobilio, S. (1985). Extended X-ray-absorption fine-structure and near-edge-structure studies on evaporated small clusters of Au. *Phys. Rev. ser. B,* **31**, 5058-5065.

Barbas, C. F., Rosenblum, J. S. & Lerner, R. A. (1993). Direct selection of antibodies that coordinate metals from semisynthetic combinatorial libraries. *Proc. Natl Acad. Sci. USA,* **90**, 6385-6389.

Belcher, A. M., Wu, X. H., Christiansen, R. J., Hansma, P. K., Stuckey, G. D. & Morse, D. E. (1996). Control of crystal phase switching and orientation by soluble mollusc-shell proteins. *Nature,* **381**, 56-58.

Brown, S. (1992). Engineered iron oxide adhesion mutants of the λ-receptor. *Proc. Natl Acad. Sci. USA,* **89**, 8651-8655.

Brown, S. (1997). Metal recognition by repeated polypeptides. *Nature Biotechnol,* **15**, 269-272.

Cleveland, C. L., Landman, U., Shafigullin, M. N., Stephens, P. W. & Whetten, R. L. (1997). Structural evolution of larger gold clusters. *Z. Phys. sect. D,* **40**, 503-508.

DeOliveira, D. B. & Laursen, R. A. (1997). Control of calcite crystal morphology by a peptide designed to bind to a specific surface. *J. Am. Chem. Soc.* **119**, 10627-10631.

Ducancel, F., Boulain, J.-C., Trémeau, O. & Ménez, A. (1989). Direct expression in *E. coli* of a functionally active protein A-snake toxin fusion protein. *Protein Eng.* **3**, 139-143.

Falini, G., Albeck, S., Weiner, S. & Addadi, L. (1996). Control of aragonite or calcite polymorphism by mollusc shell macromolecules. *Science,* **271**, 67-69.

Fersht, A. (1998). *Structure and Mechanism in Protein Science*, W.H. Freeman and Co., New York.

Fincham, A. G., Moradian-Oldak, J. & Simmer, J. P. (1999). The structural biology of the developing dental enamel matrix. *J. Struct. Biol.* **126**, 270-299.

Fire, A. & Xu, S.-Q. (1995). Rolling replication of short DNA circles. *Proc. Natl Acad. Sci. USA,* **92**, 4641-4645.

Flores, C., Vazquez, A. & Hernández-Reyes, R. (1998). Size and shape distributions in gold colloidal particles. In *Electron Microscopy 1998. Proceedings of the 14th International Congress on Electron Microscopy* (Calderon, H. & Yacaman, M. J., eds), pp. 425-426, Springer-Verlag, Germany.

Geddes, N. J., Martin, A. S., Caruso, F., Urquhart, R. S., Furlong, D. N., Sambles, J. R., Than, K. A. & Edgar, J. A. (1994). Immobilisation of IgG onto gold surfaces and its interaction with anti-IgG studied by surface plasmon resonance. *J. Immunol. Methods,* **175**, 149-160.

Handley, D. A. (1989). Methods for synthesis of colloidal gold. In *Colloidal Gold: Principles, Methods and Applications* (Hayat, M. A., ed.), vol. 1, pp. 13-32, Academic Press, San Diego.

Huston, J. S., Levinson, D., Mudgett-Hunter, M., Tai, M. S., Novotny, J., Margolies, M. N., Ridge, R. J., Bruccoleri, R. E., Haber, E., Crea, R. & Oppermann, H. (1988). Protein engineering of antibody binding sites: recovery of specific activity in an anti-digoxin

single-chain Fv analogue produced in *Escherichia coli*. *Proc. Natl Acad. Sci. USA,* **85**, 5879-5883.

Klaus, T., Joerger, R., Olsson, E. & Granqvist, C.-G. (1999). Silver-based crystalline nanoparticles, microbially fabricated. *Proc. Natl Acad. Sci. USA,* **96**, 13611-13614.

Laemmli, U. K. (1970). Cleavage of structure proteins during assembly of the head of bacteriophage T4. *Nature,* **227**, 680-685.

Liu, D., Daubendiek, S. L., Zillmann, M. A., Ryan, K. & Kool, E. T. (1996). Rolling circle DNA synthesis: small circular oligonucleotides as efficient templates for DNA polymerases. *J. Am. Chem. Soc.* **118**, 1587-1594.

Lizardi, P. M., Huang, X., Zhu, Z., Bray-Ward, P., Thomas, D. C. & Ward, D. C. (1998). Mutation detection and single-molecule counting using isothermal rolling-circle amplification. *Nature Genet.* **19**, 225-232.

Mann, S. (1988). Molecular recognition in biomineralization. *Nature,* **332**, 119-123.

Mann, S., Didymus, J. M., Sanderson, N. P., Heywood, B. R. & Aso, Samper E. J. (1990). Morphological influence of functionalized and non-functionalized α,ω-dicarboxylates on calcite crystallization. *J. Chem. Soc. Faraday Trans,* **86**, 1873-1880.

Marks, L. D. (1994). Experimental studies of small particle structures. *Rep. Prog. Phys.* **57**, 603-649.

Mayer, A. & Antonietti, M. (1998). Investigation of polymer-protected noble metal nanoparticles by transmission electron microscopy: control of particle morphology and shape. *Colloid Polym. Sci.* **276**, 769-779.

Miller, J. H. (1972). *Experiments in Molecular Genetics*, Cold Spring Harbor Laboratory Press, Cold Spring Harbor, New York.

Newton, S. M. C., Klebba, P. E., Michel, V., Hofnung, M. & Charbit, A. (1996). Topology of the membrane protein LamB by epitope tagging and a comparison with the X-ray model. *J. Bacteriol.* **178**, 3447-3456.

Porter, D. A. & Easterling, K. E. (1992). *Phase Transformations in Metals and Alloys*, Chapman and Hall, London.

Sarikaya, M., Liu, J. & Aksay, I. A. (1995). Nacre: properties, crystallography and formation. In *Biomimetics: Design and Processing of Materials* (Sarikaya, M. & Aksay, I. A., eds), pp. 35-90, AIP, New York.

Simkiss, K. & Wilbur, K. M. (1989). *Biomineralization*, Academic Press, New York.

Simmer, J. P. & Fincham, A. G. (1995). Molecular mechanisms of dental enamel formation. *Crit. Rev. Oral. Biol. Med.* **6**, 84-108.

Southam, G. & Beveridge, T. J. (1994). The *in vitro* formation of placer gold by bacteria. *Geochem. Cosmochem. Acta,* **58**, 4527-4530.

Stathis, E. C. & Fabrikanos, A. (1958). Preparation of colloidal gold. *Chem. Ind.* **47**, 860-861.

Turkevich, J., Stevenson, P. C. & Hillier, J. (1951). A study of the nucleation and growth processes in the synthesis of colloidal gold. *Trans. Faraday. Soc. Disc.* **11**, 55-75.

Weissbuch, I., Addadi, L., Lahav, M. & Leiserowitz, L. (1991). Molecular recognition at crystal interfaces. *Science,* **253**, 637-645.

Wells, J. A. (1996). Hormone mimicry. *Science,* **273**, 449-450.

Williams, D. B. & Carter, C. B. (1996). *Transmission Electron Microscopy*, Plenum Press, London and New York.

Edited by M. Gottesman

(Received 10 December 1999; received in revised form 2 March 2000; accepted 8 March 2000)